Nanoparticle delivery of immunostimulatory oligonucleotides enhances response to checkpoint inhibitor therapeutics

As Published: 10.1073/PNAS.2001569117

Publisher: Proceedings of the National Academy of Sciences

Persistent URL: https://hdl.handle.net/1721.1/134619

Version: Final published version: final published article, as it appeared in a journal, conference proceedings, or other formally published context

Nanoparticle delivery of immunostimulatory oligonucleotides enhances response to checkpoint inhibitor therapeutics

Colin G. Buss[a,b] and Sangeeta N. Bhatia[a,b,c,d,e,f,g,1]

[a]Harvard–MIT Health Sciences and Technology Program, Institute for Medical Engineering and Science, Massachusetts Institute of Technology, Cambridge, MA 02139; [b]Koch Institute for Integrative Cancer Research, Massachusetts Institute of Technology, Cambridge, MA 02139; [c]Department of Electrical Engineering and Computer Science, Massachusetts Institute of Technology, Cambridge, MA 02139; [d]Department of Medicine, Brigham and Women's Hospital and Harvard Medical School, Boston, MA 02115; [e]Broad Institute of Massachusetts Institute of Technology and Harvard University, Cambridge, MA 02139; [f]Howard Hughes Medical Institute, Chevy Chase, MD 20815; and [g]Wyss Institute at Harvard University, Boston, MA 02115

Contributed by Sangeeta N. Bhatia, April 21, 2020 (sent for review January 29, 2020; reviewed by Rashid Bashir and Daniel A. Heller)

The recent advent of immune checkpoint inhibitor (CPI) antibodies has revolutionized many aspects of cancer therapy, but the efficacy of these breakthrough therapeutics remains limited, as many patients fail to respond for reasons that still largely evade understanding. An array of studies in human patients and animal models has demonstrated that local signaling can generate strongly immunosuppressive microenvironments within tumors, and emerging evidence suggests that delivery of immunostimulatory molecules into tumors can have therapeutic effects. Nanoparticle formulations of these cargoes offer a promising way to maximize their delivery and to enhance the efficacy of checkpoint inhibitors. We developed a modular nanoparticle system capable of encapsulating an array of immunostimulatory oligonucleotides that, in some cases, greatly increase their potency to activate inflammatory signaling within immune cells in vitro. We hypothesized that these immunostimulatory nanoparticles could suppress tumor growth by activating similar signaling in vivo, and thereby also improve responsiveness to immune checkpoint inhibitor antibody therapies. We found that our engineered nanoparticles carrying a CpG DNA ligand of TLR9 can suppress tumor growth in several animal models of various cancers, resulting in an abscopal effect on distant tumors, and improving responsiveness to anti-CTLA4 treatment with combinatorial effects after intratumoral administration. Moreover, by incorporating tumor-homing peptides, immunostimulatory nucleotide-bearing nanoparticles facilitate antitumor efficacy after systemic intravenous (i.v.) administration.

nanoparticle | immunotherapy | oiligonucleotides | cancer

Despite decades of advances in cancer treatment, contributing to a ∼1 to 2% decrease in death rates from cancer between 1982 and 2015, cancer was estimated to have killed more than 600,000 Americans in 2019 (1). The advent of immune checkpoint inhibitor therapies (e.g., CTLA-4 and PD-1/PD-L1 antibodies) has revolutionized cancer treatment, but efficacy is limited, with overall objective response rates limited to 15 to 20% of patients (2–4). The reasons for this limitation remain an area of great interest and active investigation (5), though emerging evidence suggests tumor mutational burden, often driven by microsatellite instability, can predict responsiveness to these treatments (6). In addition, an array of studies in human patients and in animal models has shown that many tumors have highly immunosuppressive microenvironments, driven by cancer cell signaling as well as antiimmunogenic signals derived from tumor-associated macrophages and other nonparenchymal cells (7–11).

Many efforts to overcome immunotherapy treatment limitations have focused on combination therapies, namely supplementing checkpoint inhibitor antibody treatment with one of an array of conventional treatment techniques including chemotherapy, genomically targeted drug therapy, radiation therapy, and therapies to enhance immune activation (12–14). These multiarm therapeutic regimens have shown varying degrees of success, and many are under active investigation in preclinical models or clinical trials (12–19). Typically, any enhanced effectiveness observed via these combined mechanisms is thought to be due to enhancing the immunogenicity of tumors and increased presentation of tumor antigens (12, 20). Evidence has emerged that the combination of immunotherapies with direct-acting, immunostimulatory molecules can enhance responsiveness to checkpoint inhibitor therapeutics, likely by abrogating immunosuppressive signaling within the tumor (14, 21). Previous studies have investigated the effects of oligonucleotide ligands of various immune receptors, STING agonists, and even biological agents such as bacteria and viruses (22–27). Several of these candidates have advanced to various stages of clinical trials with varying degrees of success (28–32), including a recently announced failure to meet the primary endpoint in a randomized phase III trial of an engineered TLR9 agonist (33). Thus far, minimally effective outcomes have been the primary reports arising from these efforts, and it appears that impediments to nucleotide delivery to optimal physical sites may be responsible for the low-level efficacy observed (34), generating great interest

Significance

Checkpoint inhibitor (CPI) immunotherapies have revolutionized the treatment of a wide array of cancers, but their utility remains limited to a subset of patients with favorable disease phenotypes. We show that the generation of peptide-based nanocomplexes carrying immunostimulatory oligonucleotides dramatically increases the potency of certain of these compounds to stimulate toll-like receptor signaling. The administration of immunostimulatory nanocomplexes carrying CpG oligonucleotides generates antitumor effects and enhances the efficacy of checkpoint inhibitor antibody therapy in mouse models of cancer, and the nanocomplex formulation enables drastic reductions in the dose required to generate therapeutic effects.

Author contributions: C.G.B. and S.N.B. designed research; C.G.B. performed research; and C.G.B. and S.N.B. wrote the paper.

Reviewers: R.B., University of Illinois at Urbana–Champaign; and D.A.H., Memorial Sloan Kettering Cancer Center.

Competing interest statement: S.N.B. holds equity in Glympse Bio and Impilo Therapeutics, is a director at Vertex, consults for Cristal, Maverick, and Moderna, and receives sponsored research funding from Johnson & Johnson.

[1]To whom correspondence may be addressed. Email: sbhatia@mit.edu.

This article contains supporting information online at https://www.pnas.org/lookup/suppl/doi:10.1073/pnas.2001569117/-/DCSupplemental.

First published June 3, 2020.

in utilizing nanoparticles and other carriers to enhance delivery of and immunostimulation by these molecules. Such methods have shown enhancement of therapeutic responses by driving accumulation of immunostimulators in specific organs and within specific cellular compartments, and by increasing receptor signaling while simultaneously decreasing systemic side effects (19, 22, 28, 34–38).

Previous work from our group has shown that rationally designed tandem peptides can encapsulate nucleic acid cargoes and facilitate their targeted delivery to various cancer types (39, 40). Prior applications of this technology have been primarily focused on the delivery of siRNA intended to suppress specific cancer-promoting transcripts (41–44). We hypothesized that this technology may also be amenable to the delivery of nucleic acid ligands of various immune receptors. Given previous evidence that nanoparticle formulation of immunostimulants may enhance their ability to induce inflammatory signaling (35, 38), we reasoned that such nanoparticle formulation may result in enhanced immune activation in cancer therapeutic applications. Here we show that our tandem peptide nanocomplex (TPNC) system is able to generate nanoparticle formulations of various oligoribonucleotide (ORN) and oligodeoxynucleotide (ODN) ligands of several toll-like receptors (TLRs). Nanoparticle formulations of certain oligonucleotide cargoes retain the ability to activate inflammatory signaling in vitro, and in at least one case greatly enhance the magnitude of such signaling. TPNCs carrying a CpG DNA ligand of TLR9 are able to suppress tumor growth after intratumoral administration, enhance responsiveness to a checkpoint inhibitor antibody therapeutic, and generate an abscopal effect suppressing growth of a distant tumor after local treatment. Notably, in each case the nanoparticle formulation is more effective than a matched dose of the unencapsulated ligand. Finally, the modification of immunostimulatory TPNCs by including tumor-homing peptides known to engage with different receptors within tumors (40, 45–47) enhances tumor accumulation of nanoparticles and improves immunotherapy responses after intravenous (i.v.) administration.

Results

Tandem Peptides Encapsulate Immunostimulatory Oligonucleotides in Nanocomplexes. Our goal was to build nanoparticle systems that have immunomodulatory activity. We drew inspiration from previous work in our group using tandem peptides comprised of an N-terminal myristoyl coupled to transportan, a cell penetrating peptide (48), and one of an array of C-terminal homing domains to form nanocomplexes with oligonucleotides (39, 40, 49). Based on this prior work, we hypothesized that we could form similar nanocomplexes with oligonucleotide-based immunostimulatory agents (Fig. 1*A*). To evaluate the ability to form nanocomplexes with tandem peptides and immunostimulatory oligonucleotides, we measured hydrodynamic diameters and polydispersity indices by dynamic light scattering (DLS) of particles formed with varying peptide/cargo ratios and an array of oligonucleotide cargoes. Each of six immunostimulatory oligonucleotides tested, consisting of various deoxy- and ribonucleotides and synthetic analogs thereof, formed measurable particles at several peptide/cargo ratios, and demonstrated low polydispersity under optimal conditions (Fig. 1 *B–G*, *Left*). These measurements are similar to those obtained with complexes formed with siRNA (*SI Appendix*, Fig. S1*A*), the cargo for which this tandem peptide system was originally optimized (39, 40). Transmission electron microscopy (TEM) imaging of particles formed with selected peptide/cargo ratios confirmed particle formation and demonstrated similar sizes as those measured by DLS (Fig. 1 *B–G*, *Right*). Gel electrophoresis confirmed complete encapsulation of cargo for each cargo tested (*SI Appendix*, Fig. S1 *B–D*). Single-stranded polyuridine (ssPolyU) cargo was not tested in gel electrophoresis as the gel stain did not interact strongly with this material. These data suggest that tandem peptides are capable of efficiently encapsulating an array of single- and double-stranded immunostimulatory oligonucleotide cargoes with varying physicochemical properties into nanocomplexes, which we term immunostimulatory tandem peptide nanocomplexes (iTPNCs).

iTPNCs Stimulate Inflammatory Signaling in Macrophages in a Particle-Dependent Manner. Once we confirmed that tandem peptides can encapsulate these various oligonucleotide cargoes, we sought to determine whether each cargo would maintain its capacity to induce immunostimulatory responses by a relevant cell population when formulated in iTPNCs. We tested iTPNCs on J774A.1 murine macrophages and queried their response to stimulation by conducting qRT-PCR for various inflammatory genes, 6 h after nanoparticle administration. Measurement of mRNA levels of *Il-6*, *Tnf-α*, *iNos*, and *Arg1* after administration of 25 nM immunostimulatory cargo (ODN 1585, ODN 1826, ODN 2395, ORN Sa19), or 3.125 μg/mL ssPolyU, or 2 μg/mL polyinosinic:polycytidylic acid (poly[I:C]), each encapsulated within iTPNCs, revealed a stimulation pattern consistent with classical immune axis activation (*Il-6*, *Tnf-α*, and *iNos*). In parallel, we observed moderate suppression of an alternative activation marker, *Arg1*, in response to a subset of the immunostimulatory cargoes, as shown by gene expression fold changes (expression after immunostimulatory treatment, relative to expression in untreated cells) (*SI Appendix*, Fig. S2*A*). Controls (tandem peptide alone, TPNCs carrying siRNA against luciferase, or TPNCs carrying sequence control nucleic acids) showed minimal effects on these inflammatory genes (*SI Appendix*, Fig. S2*A*). Comparing gene expression fold changes by z-score across each gene, we observed that of the immunostimulatory cargoes tested, ODN 1826 (class B Tlr9 ligand) and ORN Sa19 (Tlr13 ligand) nanoparticles most effectively activate inflammatory signaling within macrophages, achieving stimulation comparable to that of lipopolysaccharide (LPS), which is a potent activator of macrophages (Fig. 2*A* and *SI Appendix*, Fig. S2*A*). Given these gene expression results, alongside the formation of more consistent nanoparticles seen with ODN 1826 relative to ORN Sa19 (Fig. 1 *C* and *G*, and *SI Appendix*, Fig. S1 *C* and *D*), and considering the ongoing clinical trials that incorporate various ligands of Tlr9, we chose to focus on ODN 1826 for the remainder of these studies.

Encouraged by the successful stimulation of macrophage inflammatory genes using ODN 1826 packaged in iTPNCs, we sought to compare the efficacy of nanoparticle-formulated ODN 1826 relative to the unencapsulated ODN. Notably, particle-formulated ODN 1826 stimulated much more robust *Il-6* gene expression than did treatment with a matched dose of the unencapsulated oligo at 6 h posttreatment over a range of concentrations (Fig. 2*B* and *SI Appendix*, Fig. S2*B*). We next aimed to determine the dose responsiveness and longevity of the gene activation by ODN 1826 iTPNCs. We again treated J774A.1 macrophages with various concentrations of ODN 1826 encapsulated within iTPNCs and measured *Il-6* mRNA levels 18 h later. As little as 3.125 nM of ODN 1826 within particles was able to robustly stimulate inflammatory gene expression at this time point, and expression levels were dose dependent (Fig. 2*C*). As an example of cell type specificity, neither particle-formulated nor unencapsulated ODN 1826 had any effect on *Il-6* gene expression by murine cancer cell lines (*SI Appendix*, Fig. S2 *C* and *D*).

iTPNCs Suppress Tumor Growth in Multiple Immunocompetent Mouse Models. Given that iTPNCs carrying ODN 1826 Tlr9 ligand robustly stimulate inflammatory gene expression within macrophages in vitro, and the established pattern that macrophages and other immune cells generate immunosuppressive and protumorigenic

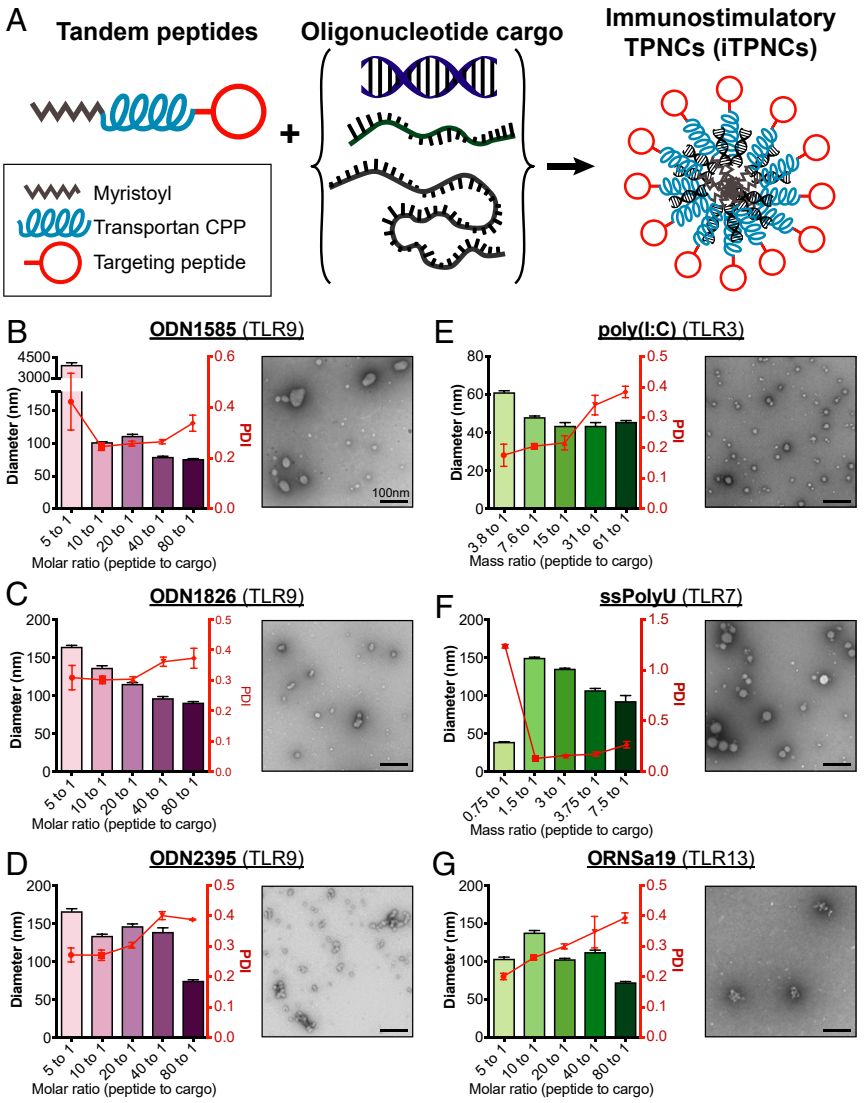

Fig. 1. Tandem peptides encapsulate immunostimulatory oligonucleotides in nanocomplexes. (*A*) Schematic of iTPNC formation with various oligonucleotide cargoes encapsulated with targeted tandem peptides. (*B–D*) DLS measurements (*Left*) of hydrodynamic diameter (purple bars) and polydispersity index (PDI, red curves) and TEM images (*Right*) of iTPNCs formulated with oligodeoxyribonucleotide TLR9 ligands ODN 1585 (*B*), ODN 1826 (*C*), and ODN 2395 (*D*) encapsulated with various ratios of peptide to cargo. (*E–G*) DLS measurements (*Left*) of hydrodynamic diameter (green bars) and PDI (red curves) and TEM images (*Right*) of iTPNCs formulated with oligoribonucleotide TLR ligands poly(I:C) (*E*), ssPolyU (*F*), and ORN Sa19 (*G*) encapsulated with various ratios of peptide to cargo. (Scale bars, 100 nm.)

signals within tumors (9, 50), we hypothesized that delivery of iTPNCs into tumors could have a growth suppressive effect. To investigate this possibility in a manner independent of delivery route and systemic effects of immunostimulation, we administered ODN 1826 iTPNCs directly into subcutaneous (s.c.) flank tumors or mammary fat pad tumors in immunocompetent mice. In flank tumors derived from B16F10 melanoma, we observed an ~40 to 50% reduction in tumor growth after several intratumoral injections of iTPNCs, relative to an equivalent dose of unencapsulated ODN 1826 (Fig. 3 *A–C* and *SI Appendix*, Fig. S3*A*). Comparable results were obtained when the treated tumors were derived from MC38 colon cancer (*SI Appendix*, Fig. S3 *C* and *D*) or 4T1 breast adenocarcinoma (*SI Appendix*, Fig. S3 *E* and *F*) cell lines, in which tumor growth was significantly suppressed with ODN 1826 iTPNCs relative to TPNCs complexed with sequence control oligonucleotides. Importantly, even after seven intratumoral injections into bilateral s.c. B16F10 tumors, we saw no evidence of systemic toxicity or weight loss (*SI Appendix*, Fig. S3*B*).

iTPNCs Enhance Responsiveness to Anti-CTLA4 Checkpoint Inhibitor Antibody Therapy after Systemic Administration. Once we established that ODN 1826 iTPNCs could suppress tumor growth, we sought to test whether homing peptides could direct the iTPNCs into tumors after systemic administration, to facilitate antitumor effects without requiring direct intratumoral injection. We initiated B16F10 tumors in mice and allowed the tumors to grow to ~100 to 150 mm^3, then injected fluorescent ODN 1826 iTPNCs synthesized with various homing peptides (CRV, LyP1, or iRGD) or a nonhoming control peptide (ARAL) i.v. and allowed the particles to circulate for 30 min before resecting the tumors and measuring fluorescence signal. We quantified nanoparticle fluorescence within the explanted tumors and saw approximately two- to threefold more nanoparticle signal in tumors from mice injected with tumor-homing CRV-, LyP1-, or iRGD-iTPNCs, relative to the nonhoming control ARAL-iTPNCs (Fig. 4*A* and *SI Appendix*, Fig. S4*A*).

We hypothesized that the increased iTPNC accumulation we observed might enhance responsiveness to checkpoint inhibitor

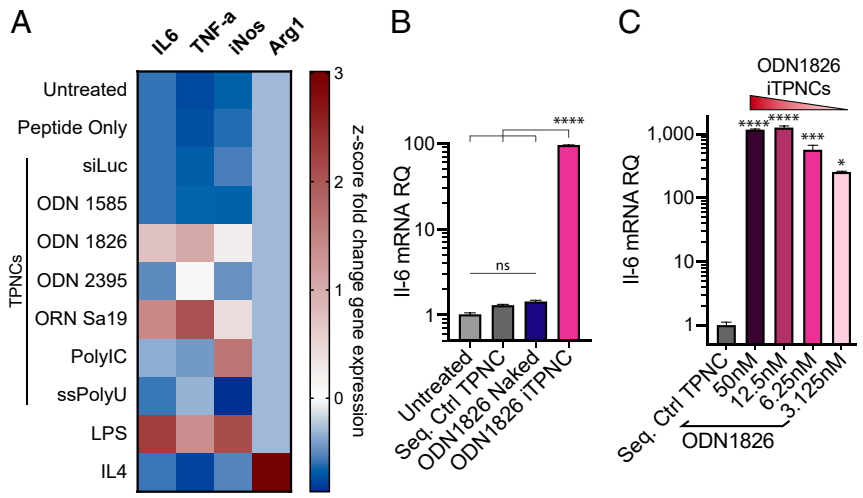

Fig. 2. TPNCs stimulate inflammatory signaling in macrophages in a particle-dependent manner. (*A*) J774A.1 murine macrophages were treated with iTPNCs carrying various TLR ligand oligonucleotide cargoes or controls (peptide only, TPNCs carrying siRNA against luciferase, 10 ng/mL LPS, or 20 ng/mL IL-4), then various genes involved in inflammatory signaling were measured by qRT-PCR 6 h later. Heatmap shows z-score values of fold change in expression of each gene relative to untreated cells. Il-6, Tnf-α, and iNos are associated with inflammatory signaling and Arg1 is associated with inhibitory signaling in macrophages. (*B*) J774A.1 macrophages were treated with 6.25 nM ODN 1826 within iTPNCs (pink bar) or without carrier (blue), or with sequence control particles. Expression of Il-6 mRNA was then measured 6 h later by qRT-PCR and shown relative to expression in untreated cells. (ns, not significant, $****P < 0.0001$, one-way ANOVA with Tukey's multiple comparisons test). (*C*) J774A.1 macrophages were treated with various concentrations of ODN 1826 or sequence control ODN formulated within iTPNCs. Expression of Il-6 mRNA was then measured 18 h later by qRT-PCR and shown relative to expression in cells treated with sequence control particles ($*P < 0.05$, $***P < 0.001$, $****P < 0.0001$, one-way ANOVA with Dunnett's multiple comparisons test).

therapeutics. To test this hypothesis, we first initiated B16F10 tumors in mice, then treated the animals with a checkpoint inhibitor antibody (anti-CTLA4) in combination with i.v. injection of unencapsulated ODN 1826, or ODN 1826 iTPNCs. The iTPNCs were synthesized with ARAL control peptide, or one of CRV, LyP1, or iRGD tumor-homing peptides. Monitoring tumor size over time revealed that tumor growth was most suppressed in mice treated with the combination of anti-CTLA4 and tumor-homing ODN 1826 iTPNCs (Fig. 4 *B* and *C* and *SI Appendix*, Fig. S4*C*). Notably, none of the injected mice showed signs of systemic toxicity or weight loss (*SI Appendix*, Fig. S4*B*). In this tumor model, we observed similar tumor suppression across the groups injected with each homing peptide-containing iTPNCs; therefore, we chose to move forward with LyP1 for the remainder of our studies.

iTPNCs Suppress Tumor Growth via an Abscopal Effect. Recent reports have found that a collection of locally administered therapeutics successfully generate abscopal effects—the phenomenon initially described in radiation therapy in which local treatment of a tumor generates shrinkage of distant nontreated tumors (51)—when used in combination with immunotherapies (24, 52–55). On this basis, we sought to test whether local administration of ODN 1826 iTPNCs could generate systemic effects without requiring i.v. injection of immunostimulatory particles. To test this hypothesis, we grew bilateral B16F10 tumors in mice and then initiated treatment intraperitoneally with anti-CTLA4. The treated mice then received an intratumoral injection into only one of the two tumors, such that two cohorts were treated with either unencapsulated ODN 1826 or ODN 1826 packaged in iTPNCs (Fig. 5*A*). Beginning anti-CTLA4 therapeutics at a very early time point, when tumors are small, allows the dose of unencapsulated ODN 1826 administered here to enhance checkpoint inhibitor treatment in a manner comparable to ODN 1826 iTPNCs, allowing us to meaningfully compare systemic effects of local treatment between these two therapeutic regimens. After its initiation, anti-CTLA4 treatment was continued for the remainder of the experiment, and intratumoral injections were repeated three times per week, into only the ipsilateral tumor of each mouse, leaving the contralateral tumors uninjected. Tumor volumes were measured and the relative final tumor volume (fold

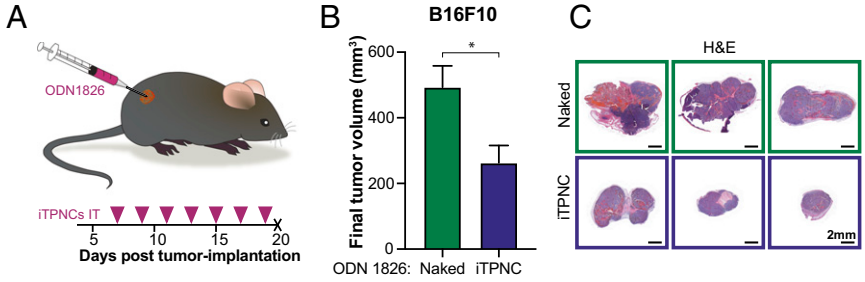

Fig. 3. iTPNCs suppress tumor growth. (*A*) Schematic and timeline for intratumoral injections. S.c. flank B16F10 murine melanoma tumors were injected intratumorally with ODN 1826 naked or formulated in iTPNCs (0.2 nmol ODN per injection) and tumors were measured over time. Tumors were injected on days indicated by pink arrowheads. (*B*) Bars show average final tumor volume at experimental endpoint on day 20 for each treatment group. ($*P = 0.0155$, unpaired *t* test; $n = 8$ tumors per group, data are representative of three independent experiments). (*C*) Images of H&E-stained sections of representative tumors from *B*. (Scale bars, 2 mm.)

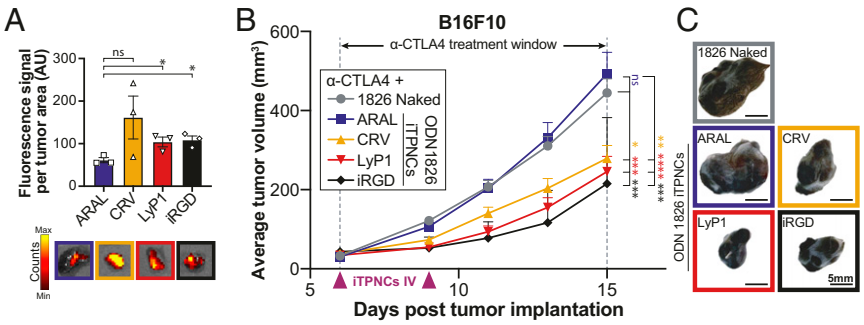

Fig. 4. iTPNCs enhance responsiveness to anti-CTLA4 checkpoint inhibitor antibody therapy after systemic administration. (*A*) Fluorescence signal from iTPNCs synthesized with various homing peptides (CRV, LyP2, or iRGD) or nonhoming control peptide (ARAL) within B16F10 tumors after i.v. injection, measured by IVIS with excitation wavelength 535 nm and emission wavelength 580 nm. *Bottom* images show simultaneously captured fluorescent images overlaid on photos of representative tumors of each treatment group (*$P < 0.05$, unpaired *t* test). (*B*) Mice bearing B16F10 tumors were treated i.v. with ODN 1826 either naked or encapsulated in iTPNCs synthesized with homing peptides (CRV, LyP1, or iRGD) or nonhoming control peptide (ARAL), and were simultaneously treated intraperitoneally with 200 μg weekly of anti-CTLA4 (during the time window indicated). Treatments were initiated when tumors reached ~30 mm^3. Curves represent average tumor volume of B16F10 tumors from each treatment group: ODN 1826 naked (gray circles), ARAL-iTPNCs (blue squares), CRV-iTPNCs (gold triangles), LyP1-iTPNCs (red triangles), or iRGD-iTPNCs (black diamonds). (ns, not significant, *$P < 0.05$, **$P < 0.01$, ***$P < 0.001$, ****$P < 0.0001$, two-way ANOVA; $n = 18$ to 20 tumors per group, error bars ± SEM, data are representative of at least two independent experiments). (*C*) Images of representative tumors from each treatment group shown in *B*. (Scale bars, 5 mm.)

change over tumors from mice treated with only anti-CTLA4) showed similar, significant, tumor suppression in the ipsilateral tumor between unencapsulated ODN 1826 and ODN 1826 iTPNCs. When the contralateral tumors were compared, however, growth suppression was only observed in the mice that received ODN 1826 iTPNC treatment (~50% tumor suppression in the distant tumor; Fig. 5 *B* and *C*), whereas the growth suppression of the contralateral tumors in unencapsulated ODN 1826-treated mice was minimal. To verify that these effects were not tumor-type or cell-line dependent, we conducted similar experiments in mice bearing bilateral MC38 colon cancer tumors. Results from experiments in which s.c. MC38 tumors were injected intratumorally with control TPNCs, unencapsulated ODN 1826, or ODN 1826 iTPNCs showed similar results as in the case of B16F10 melanoma tumors. Comparing the relative final tumor volume (fold change over tumors from mice treated with IgG) showed that ODN 1826 iTPNCs generated a significant abscopal effect, whereas unencapsulated ODN 1826 did not (*SI Appendix*, Fig. S5).

Combined iTPNC and Anti-CTLA4 Treatment Regimen Achieves Synergistic Tumor Suppression. Based on the successful enhancement of checkpoint inhibitor therapy via i.v. or intratumoral administration of ODN 1826 iTPNCs, we sought to evaluate whether frequent dosing with iTPNCs could positively impact anti-CTLA4 treatment of more advanced tumors. To this end, we injected ODN 1826 iTPNCs or sequence control TPNCs into B16F10 tumors while simultaneously treating the tumor-bearing mice with systemic injections of anti-CTLA4 or IgG isotype control antibody. We initiated therapeutics when the tumors reached ~30 to 40 mm^3, since at this size, the same dose of unencapsulated ODN 1826 was not effective (*SI Appendix*, Fig. S6; intratumoral injection of ~20 mm^3 B16F10 tumors three times per week with unencapsulated ODN 1826 in combination with anti-CTLA4). While only moderate effects of anti-CTLA4 treatment alone were observed on average tumor volume measurements in this tumor model, significant, virtually complete tumor growth arrest was achieved in mice that received combination therapy of anti-CTLA4 with ODN 1826 iTPNCs (Fig. 6*A*). Individual tumor growth curves show that a small proportion of tumors respond

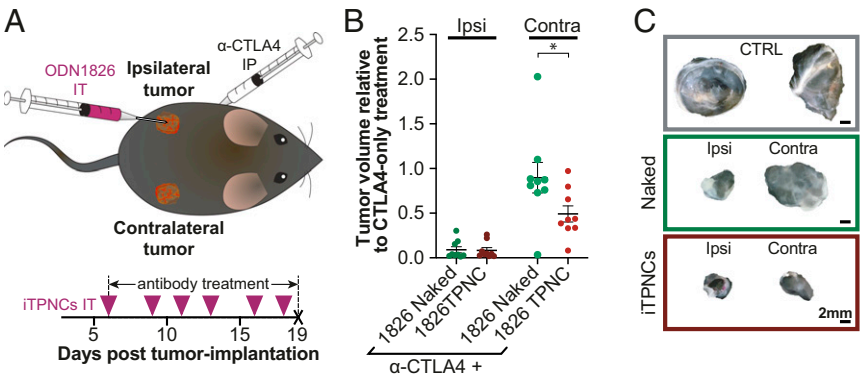

Fig. 5. iTPNCs suppress tumor growth via an abscopal effect. (*A*) Schematic of experimental design to test abscopal effects. Anti-CTLA4 checkpoint inhibitor antibody was administered intraperitoneally into each mouse bearing bilateral B16F10 s.c. flank tumors. Unencapsulated ODN 1826 (naked), or ODN 1826 iTPNCs were injected intratumorally into the ipsilateral (Ipsi) tumor, and both the ipsilateral and contralateral (Contra) tumors were measured. Tumors were injected on days indicated by pink arrowheads, and antibody treatment was continued for the length of the study. (*B*) Plots show the final tumor volume relative to tumors in mice treated only with anti-CTLA4 antibody. The two *Left* plots show the volume of the ipsilateral, intratumorally injected tumor, and the two *Right* plots show the volume of the contralateral, noninjected tumor. (*$P = 0.0337$, one-way ANOVA with Tukey's multiple comparisons test, $n = 9$ tumors per group, error bars ± SEM, data are representative of three independent experiments). (*C*) Representative images of tumors from each of the treatment groups from *B*. (Scale bars, 2 mm.)

robustly when treated with anti-CTLA4 and nonimmunostimulatory control TPNCs, whereas no mice treated with anti-CTLA4 in combination with ODN 1826 iTPNCs experience significant tumor growth (Fig. 6*B*). Representative hematoxylin and eosin-stained histology sections from each treatment group illustrate the magnitude of the combination therapy effect (Fig. 6*C*). Importantly, no treatment group showed signs of systemic toxicity or weight loss (*SI Appendix*, Fig. S7), suggesting these combination therapies are well tolerated by mice under the conditions tested. Similar experiments in mice bearing larger (70 mm^3 average volume) MC38 colon cancer tumors confirmed that this combination effect is not specific to the tumor type or cell line (*SI Appendix*, Fig. S8 *A–D*).

Discussion

Here, we generated a modular nanoparticle system for the delivery of immunostimulatory nucleic acids to tumors, in order to enhance responsiveness to immune checkpoint inhibitor antibodies—therapeutics with immense potential for dramatic efficacy in cancer treatment, but that are limited by relatively poor individual response rates within the patient pool (2, 4). Together, our data demonstrate that encapsulation of TLR ligands within nanoparticles can enhance their efficacy both in inducing inflammatory signaling in vitro, and also in suppressing tumor growth in multiple tumor models in vivo. These data also illustrate that iTPNCs can dramatically improve tumor responsiveness to checkpoint inhibitor therapeutics after i.v. or intratumoral administration, and can additionally generate an abscopal effect—showing suppression of tumor growth at a site distant from the intratumoral treatment.

This work builds upon a number of previous studies that demonstrate the efficacy of various TLR and other immune receptor ligands when administered both alone and in combination with other immunotherapies for the treatment of cancer. Of note, encapsulation of ODN 1826 into this nanoparticle formulation allows us to see effects at much lower doses (10- to 200-fold lower) than those administered in previous studies using intra- or peritumoral delivery. It is likely that the enhancement of immunostimulation seen with iTPNC formulation of ODN 1826 relative to nonencapsulated ODN results from more efficient localization of the immunostimulant within the endolysosomal compartment (35), where Tlr9 is most abundantly expressed (56–58). Such dose reduction strategies are important considerations, as they are thought to minimize the risk of off-target immune activation and various other side effects associated with systemic inflammatory signaling, which can be detrimental to cancer treatment by resulting in premature cessation of therapy in response to immune-related adverse events (12, 59, 60).

We studied ODN 1826 most extensively in this proof-of-principle work based on its physicochemical properties in nanoparticle formulation and its activation of murine J774A.1 macrophages. While this iTPNC formulation generated robust tumor-suppressive results, it is possible that other formulations—such as those encapsulating alternative immunostimulatory ligands—may also prove effective. We expect that iTPNCs—based on their homing peptides (LyP1 and CRV both direct nanoparticles into tumor macrophages) (45, 61) and their physicochemical properties—should interact strongly with macrophages, but may succeed in delivering immunostimulatory cargoes to other antigen-presenting cells such as dendritic cells (DCs), and in so doing could also result in tumor suppression effects. Thus, additional nanoparticle cargoes, such as alternative classes of CpG DNAs, may activate other cell types in vivo, even if they failed to robustly activate macrophage cell lines in our initial in vitro screen.

Based on prior characterization of the homing peptides incorporated into the tandem peptides used to form iTPNCs in this study, and on our previous success in achieving siRNA accumulation in macrophages via TPNCs and other nanoparticles with similar physicochemical properties, we expect the tumor suppressive and checkpoint inhibitor (CPI)-potentiation effects seen here to be mediated largely by macrophages. However, TLR9 is expressed by various other immune cells, including certain subsets of DCs and T cells, and signaling through these other cell populations could have an impact on antitumor responses (62–64). It is therefore possible that the effects of iTPNC treatment could be mediated through engagement of TLRs on alternate immune cells, rather than being a purely macrophage-dependent response.

A particularly exciting aspect of this modular nanoparticle technology is the ability to incorporate additional treatment strategies in a simple manner. In this work, we demonstrate the delivery of one immunostimulatory oligonucleotide into tumors to generate an antitumor response and potentiate checkpoint inhibitor therapeutic. Notably, the technology described here could also be expanded to incorporate other immunostimulatory cargoes, either alone or in combination, that act through orthogonal

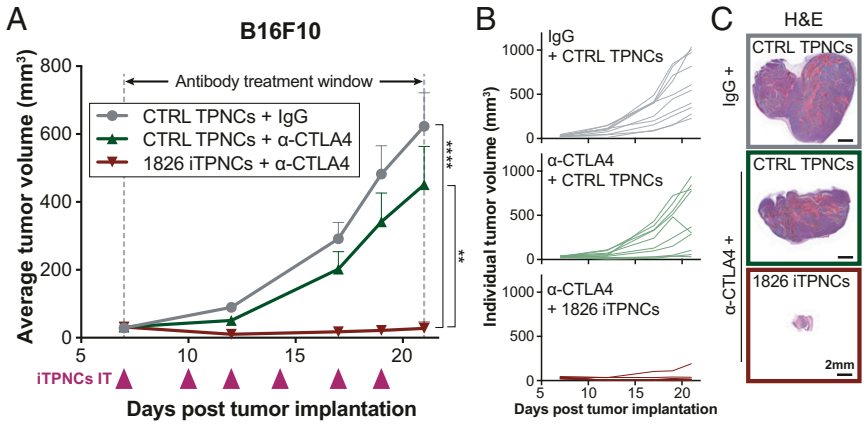

Fig. 6. Combined iTPNC and anti-CTLA4 treatment regimen achieves synergistic tumor suppression. (*A*) S.c. flank B16F10 murine melanoma tumors were injected intratumorally with ODN 1826 iTPNCs or TPNCs carrying sequence control ODN (0.2 nmol ODN per injection), and mice were concurrently treated with either IgG isotype control antibody or anti-CTLA4 checkpoint inhibitor antibody (200 μg per week injected intraperitoneally, during time window indicated). Curves show tumor volume in mice treated with IgG + sequence control TPNCs (gray circles), anti-CTLA4 + sequence control TPNCs (green triangles), or anti-CTLA4 + ODN 1826 iTPNCs (red triangles). (**P = 0.0013, ****P < 0.0001, two-way ANOVA, n = 10 tumors per group, error bars ± SEM, data are representative of three independent experiments). (*B* and *C*) Individual tumor growth curves (*B*) and images of H&E-stained sections from representative tumors (*C*) for each of the groups shown in *A*. (Scale bars, 2 mm.)

signaling pathways. Activating signaling through multiple toll-like receptors, for example, could result in enhanced immune activation. The modularity of iTPNCs also offers the potential to direct immunostimulatory therapeutics to various cell types of interest such as dendritic cells, by modifying the homing peptides used in nanoparticle synthesis (65). Given the likely trafficking of these nanoparticles into antigen presenting cells, another attractive future application of such nanotechnology could be in combination with cancer vaccination techniques, by delivering tumor antigens within the same nanoparticles. The promising results of previous studies incorporating immunostimulatory ligands, including CpG ODNs, with cancer antigens (18, 35, 37) suggest this could be a successful strategy to even more robustly stimulate an antitumor response.

Overall, the work described here demonstrates the power of this nanotechnology to overcome challenges faced by checkpoint inhibitor therapeutics by increasing the local potency of immunostimulatory cargoes, ultimately resulting in dramatic tumor growth suppression. These results are likely driven by a number of factors, including nanoparticle encapsulation resulting in protection of cargoes from degradation prior to reaching their cellular targets, directing cargoes to cells of interest, and driving accumulation of cargoes in specific subcellular compartments. Our results demonstrate that formulating oligonucleotide immunostimulants within nanoparticles facilitates dramatic tumor suppression in combination with checkpoint inhibitors at doses much lower than are effective in unencapsulated form, and can drive accumulation of cargoes in tumors in a manner dependent upon their homing properties. This effect allows us to overcome delivery challenges common in many studies of anticancer therapeutics, including immunostimulatory agents, without being limited to direct intratumoral administration.

Materials and Methods

Cell Culture. MC38 cells were purchased from Kerafast. The 4T1, B16F10, and J774A.1 cells were purchased from the American Type Culture Collection. Each cell line was screened for mycoplasma prior to in vitro or in vivo use. All cells were maintained in Dulbecco's Modified Eagle Medium (DMEM) supplemented with 10% fetal bovine serum (FBS) and penicillin/streptomycin.

Tandem Peptides. Tandem peptides were purchased from CPC Scientific. Sequences are:

mTP-TAMRA-LyP1 (Myr-GWTLNSAGYLLGKINLKALAALAKKILGGGG-K(5TAMRA)-CGNKRTRGC (C-C bridge));

mTP-TAMRA-CRV (Myr-GWTLNSAGYLLGKINLKALAALAKKILGGGG-K(5TAMRA)-CRVLRSGSC (C-C bridge));

mTP-TAMRA-iRGD (Myr-GWTLNSAGYLLGKINLKALAALAKKILGGGG-K(5TAMRA)-CRGDRGPDC (C-C bridge));

mTP-TAMRA-ARAL (Myr-GWTLNSAGYLLGKINLKALAALAKKILGGGG-K(5TAMRA)-ARALPSQRSR).

PEGylated formulations of these peptides were synthesized as previously described (49). The sequences are:

mTP-PEG-LyP1 (Myr-GWTLNSAGYLLGKINLKALAALAKKILC-PEG$_{5K}$-GGG-CGNKRTRGC (C-C bridge));

mTP-PEG-CRV (Myr-GWTLNSAGYLLGKINLKALAALAKKILC-PEG$_{5K}$-GGG-CRVLRSGSC (C-C bridge));

mTP-PEG-iRGD (Myr-GWTLNSAGYLLGKINLKALAALAKKILC-PEG$_{5K}$-GGG-CRGDRGPDC (C-C bridge));

mTP-PEG-ARAL (Myr-GWTLNSAGYLLGKINLKALAALAKKILC-PEG$_{5K}$-GGG-ARALPSQRSR).

Oligonucleotides. TLR ligand oligonucleotides and their controls were purchased from InvivoGen. Sequences of oligonucleotides are:

ODN 1585 control (5′-ggGGTCAAGCTTGAgggggg-3′)

ODN 1585 (5′-ggGGTCAACGTTGAgggggg-3′)

ODN 1826 control (5′-tcc atg agc ttc ctg agc tt-3′)

ODN 1826 (5′-tccatgacgttcctgacgtt-3′)

ODN 2395 control (5′-tgctgcttttgggggggcccccc-3′)

ODN 2395 (5′-tcgtcgttttcggcgcgcgccg-3′)

ORN Sa19 control (5′-ggacgggaagaccccgugg-3′)

ORN Sa19 (5′-ggacggaaagaccccgugg-3′)

Bases in capital letters are phosphodiester and those in lowercase are phosphorothioate.

Poly(I:C) comprises short strands of polyinosine homopolymer annealed to short strands of polycytidine homopolymer, with an average size from 0.2 kb to 1 kb.

ssPolyU is a synthetic single-stranded polyuridine homopolymer.

siLuciferase was purchased from Dharmacon. The siLuc ON-TARGETplus sense sequence used is (5′-CUUACGCUGAGUACUUCGA-dT-dT-3′).

Nanoparticle Synthesis and Analysis. Nanoparticles for in vitro characterization and intratumoral administration studies were synthesized as previously described (40). Briefly, oligonucleotides were diluted in nuclease-free water. Various molar or mass ratios of peptide to cargo were mixed with each oligonucleotide and particles were allowed to stabilize for 15 min prior to analysis. For DLS measurements, samples were analyzed with a Malvern Zetasizer and average hydrodynamic diameter and polydispersity index were measured over at least five sequential runs per sample. PEGylated nanoparticles for i.v. delivery were synthesized as previously described (49). Briefly, ODN 1826 was diluted in phosphate-buffered saline (PBS). PEGylated tandem peptide (mTP-PEG-LyP1, mTP-PEG-ARAL, mTP-PEG-CRV, or mTP-PEG-iRGD) were mixed with oligonucleotide at 10× molar ratio. Finally non-PEGylated tandem peptides (mTP-LyP1, mTP-ARAL, mTP-CRV, or mTP-iRGD) were mixed with the PEG/ODN mixture at 10× molar ratio (relative to ODN). Nanoparticles were allowed to stabilize for at least 15 min, then diluted to the appropriate concentration for i.v. injection with PBS.

TEM Imaging. TPNCs were prepared with each cargo as described above. Freshly ionized carbon-coated grids were floated on a 10-μL drop of each sample for 1 min. The grid was washed with five drops of 2% acidic uranyl acetate (UA) and excess UA was drawn off with grade 50 Whatman filter paper. Grids were allowed to dry and imaged with a FEI Tecnai spirit TEM at 80 KV. Images shown were taken at 23,000× direct magnification. (Scale bars, 100 nm.)

Nanoparticle Gel Electrophoresis. Nanocomplexes were synthesized as described above, using a variety of ratios of peptide to oligonucleotide cargo. Samples of equivalent oligonucleotide content were run in a 2% agarose gel and visualized via SYBR Gold nucleic acid gel stain (Thermo Fisher) with ultraviolet (UV) transillumination.

iTPNC Inflammatory Signaling Screen. J774A.1 murine macrophages were plated in 12-well plates ~24 h prior to addition of oligonucleotides. TPNCs were prepared as described above carrying one of ODN 1585, ODN 1826, ODN 2395, ORN Sa19, poly(I:C), ssPolyU, siRNA against luciferase, or respective controls for the immunostimulatory cargoes. To query the stimulation of inflammatory genes by the various iTPNCs, 25 nM immunostimulatory cargo (ODN 1585, ODN 1826, ODN 2395, ORN Sa19), or 3.125 μg/mL ssPolyU, or 2 μg/mL poly(I:C) formulated into iTPNCs, or respective controls were added to the cell media. For the peptide-only control, the same final concentration of peptide as each of the iTPNCs was added to the cell media. For LPS control, 100 ng/mL of LPS was added to the cell media, and for IL-4 control, 20 ng/mL IL-4 was added to the cell media. Each condition was tested in triplicate. After 6 h, RNA was isolated from the cells using Norgen Total RNA Purification Kits (Norgen Biotek, Cat. No. 17200), and cDNA was synthesized using the SuperScript III First-Strand Synthesis System (Invitrogen Cat. No. 18080051). Quantitative PCR reactions were conducted using SsoFast EvaGreen Supermix (Bio-Rad Cat. No. 1725203). Each qPCR reaction was performed in triplicate, and Gapdh was used as an endogenous control. The mean cycle threshold (Ct) was used to calculate relative mRNA expression. Values depicted in heatmaps are log2(average fold change relative to untreated cells) and z-score across each gene of average fold change relative to untreated cells (calculated as [value − mean]/SD). Primers used for the qPCR reactions were:

Arg1: forward 5′-CTCCAAGCCAAAGTCCTTAGAG-3′,

reverse 5′-AGGAGCTGTCATTAGGGACATC-3′;

Il-6: forward 5′-GCTACCAAACTGGATATAATCAGGA-3′,

reverse 5′-CCAGGTAGCTATGGTACTCCAGAA-3′;

iNos: forward 5′-TTCACCCAGTTGTGCATCGACCTA-3′,

reverse 5′-TCCATGGTCACCTCCAACACAAGA-3′;

Gapdh: forward 5′-GCACAGTCAAGGCCGAGAAT-3′,

reverse 5′-GCCTTCTCCATGGTGGTGAA-3′;

Tnf-α: forward 5′-CTACTCCCAGGTTCTCTTCAA-3′,

reverse 5′-GCAGAGAGGAGGTTGACTTTC-3′.

Unencapsulated vs. iTPNC Comparison. iTPNCs carrying ODN 1826 or ODN 1826-control sequence were prepared as described above. J774A.1 macrophages were plated in 12-well plates, and treated with 6.25 nM, 12.5 nM, or 25 nM of ODN 1826 unencapsulated or within iTPNCs, or 25 nM of ODN 1826-control in TPNCs ∼24 h after plating. Each condition was tested in triplicate. After 6 h, RNA was extracted and qPCR for *Il-6* was performed as described above. *Il-6* mRNA quantifications are shown relative to untreated cells.

iTPNC Testing on Cancer Cells. B16F10 melanoma cells or 4T1 breast cancer cells were plated in 12-well plates and treated with 25 nM of ODN 1826 unencapsulated or within iTPNCs, or 25 nM of ODN 1826-control in TPNCs ∼24 h after plating. Each condition was tested in triplicate. After 6 h, RNA was extracted and qPCR for *Il-6* was performed as described above. *Il-6* mRNA quantifications are shown relative to untreated cells.

iTPNC Dose–Response Evaluation. J774A.1 macrophages were plated in 12-well plates and treated with a range of concentrations of ODN 1826 within iTPNCs, or 50 nM ODN 1826-control in TPNCs. Each condition was tested in triplicate. After 18 h, RNA was extracted and qPCR for *Il-6* was performed as described above. *Il-6* mRNA quantifications are shown relative to cells treated with ODN 1826-control TPNCs.

Animal Studies. All animal studies were approved by the Massachusetts Institute of Technology's Committee on Animal Care and were completed in accordance with the National Institutes of Health Guide for the Care and Use of Laboratory Animals. For tumor growth experiments, 6- to 8-wk-old female C57Bl6 mice or 5- to 7-wk-old female BALB/c mice (Taconic Biosciences) were implanted with 1 to 5×10^5 B16F10 murine melanoma cells or 2×10^6 MC38 murine colon adenocarcinoma cells s.c. into bilateral rear flanks (C57Bl6) or 1×10^6 4T1 murine breast cancer cells bilaterally into the mammary fat pads (BALB/c). Tumor cells were implanted in 100 uL of 30% matrigel in PBS. Tumor growth was monitored by measurement with digital calipers. Prior to initiation of therapeutic treatment, mice were randomized and tumors were measured.

Nanoparticle Therapeutic Injection Studies. For intratumoral administration of immunostimulants, nanoparticles were prepared as described above, and 0.2 nmol of oligonucleotide encapsulated within nanoparticles or unencapsulated were injected intratumorally at various time points.

For i.v. therapeutic administration experiments, PEGylated nanoparticles were prepared as described above, and 1 nmol of oligonucleotide, encapsulated within nanoparticles or unencapsulated, in 150 μL of PBS were injected into the lateral tail vein at various time points.

Checkpoint Inhibitor Antibody Therapeutics. For studies in which mice were treated with checkpoint inhibitor antibodies, 200 μg per week of anti-mouse CTLA4 (clone 9D9, BioXCell) or isotype control IgG2b (clone MPC-11, BioXCell) were injected intraperitoneally in 100 μL of PBS for the duration of the study.

Nanoparticle Tumor Accumulation Studies. For visualization of nanoparticle fluorescence within tumors, 5×10^5 B16F10 cells were injected s.c. in the flanks of C57Bl6 mice and allowed to grow. On the sixth day following tumor induction, anti-CTLA4 checkpoint inhibitor antibody was administered intraperitoneally as described above. On the seventh day following tumor induction ∼24 h after antibody administration, when the tumors had reached ∼100 to 150 mm^3, 2 nmol of ODN 1826 encapsulated within PEGylated TPNCs (formed as described above) were injected i.v. in the lateral tail veins of tumor-bearing, CTLA4-treated mice. After 30 min, mice were euthanized and tumors were explanted. Nanoparticle fluorescence signal from TAMRA-labeled particles was measured with excitation wavelength of 535 nm and emission wavelength of 580 nm using the IVIS Spectrum Fluorescent Imaging System (Perkin-Elmer). All of the tumors were imaged simultaneously in one field of view. Following image acquisition, the perimeter of each tumor was outlined using ImageJ software (NIH) to calculate cross-sectional area. Total counts in the region of interest are reported per area (fluorescence counts/cross-sectional area), and each tumor in the fluorescence images is shown with the same minimum and maximum counts, corresponding to the scale bars in Fig. 4*A* and *SI Appendix*, Fig. S4*A*.

Histology. Tumors were fixed with 10% formalin following dissection from euthanized mice. Tumors were then dehydrated, paraffin-embedded, and sectioned. For gross histological evaluation, tumor sections were stained with hematoxylin and eosin.

Statistical Analyses. All statistical analyses were performed using GraphPad Prism 8. Details of statistical tests are provided in the legend of each figure.

Data Availability. All data necessary for study replication have been included in the submission. Materials are available commercially and are listed in *Materials and Methods*.

ACKNOWLEDGMENTS. We thank the Koch Institute Swanson Biotechnology Center for technical support, specifically Kathleen Cormier in the Hope Babette Tang Histology Facility. We thank Nicki Watson (W. M. Keck Microscopy Facility at the Whitehead Institute) for her expert assistance with electron microscopy, and Dr. Ester Kwon (University of California San Diego) for reagents and fruitful discussion. We thank Dr. Heather Fleming (MIT) for critical reading and editing of the manuscript. This study was supported in part by Koch Institute Support Grant P30-CA14051 from the National Cancer Institute (Swanson Biotechnology Center); a Core Center Grant P30-ES002109 from the National Institute of Environmental Health Sciences; the Koch Institute's Marble Center for Cancer Nanomedicine; and the Ludwig Center for Molecular Oncology at MIT. C.G.B. thanks the National Science Foundation Graduate Research Fellowship Program for support. S.N.B. is a Howard Hughes Medical Institute Investigator.

1. A. Noone *et al*., *SEER Cancer Statistics Review, 1975-2015*, (National Cancer Institute, 2018).
2. C. L. Ventola, Cancer immunotherapy, Part 3: Challenges and future trends. *P&T* **42**, 514–521 (2017).
3. J. A. Seidel, A. Otsuka, K. Kabashima, Anti-PD-1 and anti-CTLA-4 therapies in cancer: Mechanisms of action, efficacy, and limitations. *Front. Oncol.* **8**, 86 (2018).
4. M. S. Goldberg, Improving cancer immunotherapy through nanotechnology. *Nat. Rev. Cancer* **19**, 587–602 (2019).
5. D. S. Chen, I. Mellman, Elements of cancer immunity and the cancer-immune set point. *Nature* **541**, 321–330 (2017).
6. R. M. Samstein *et al*., Tumor mutational load predicts survival after immunotherapy across multiple cancer types. *Nat. Genet.* **51**, 202–206 (2019).
7. V. Velcheti, K. Schalper, Basic overview of current immunotherapy approaches in cancer. *Am. Soc. Clin. Oncol. Educ. Book* **35**, 298–308 (2016).
8. P. Sharma, S. Hu-Lieskovan, J. A. Wargo, A. Ribas, Primary, adaptive, and acquired resistance to cancer immunotherapy. *Cell* **168**, 707–723 (2017).
9. D. Hanahan, R. A. Weinberg, Hallmarks of cancer: The next generation. *Cell* **144**, 646–674 (2011).
10. E. Peranzoni *et al*., Macrophages impede CD8 T cells from reaching tumor cells and limit the efficacy of anti-PD-1 treatment. *Proc. Natl. Acad. Sci. U.S.A.* **115**, E4041–E4050 (2018).
11. T. Chanmee, P. Ontong, K. Konno, N. Itano, Tumor-associated macrophages as major players in the tumor microenvironment. *Cancers* **6**, 1670–1690 (2014).
12. P. Sharma, J. P. Allison, Immune checkpoint targeting in cancer therapy: Toward combination strategies with curative potential. *Cell* **161**, 205–214 (2015).
13. S. Kruger *et al*., Advances in cancer immunotherapy 2019–Latest trends. *J. Exp. Clin. Cancer Res.* **38**, 268 (2019).
14. C. M. Fares, E. M. Van Allen, C. G. Drake, J. P. Allison, S. Hu-Lieskovan, Mechanisms of resistance to immune checkpoint blockade: Why does checkpoint inhibitor immunotherapy not work for all patients? *Am. Soc. Clin. Oncol. Educ. Book* **39**, 147–164 (2019).
15. M. Wang, Y. Liu, Y. Cheng, Y. Wei, X. Wei, Immune checkpoint blockade and its combination therapy with small-molecule inhibitors for cancer treatment. *Biochim. Biophys. Acta Rev. Cancer* **1871**, 199–224 (2019).
16. A. van Elsas, A. A. Hurwitz, J. P. Allison, Combination immunotherapy of B16 melanoma using anti-cytotoxic T lymphocyte-associated antigen 4 (CTLA-4) and granulocyte/macrophage colony-stimulating factor (GM-CSF)-producing vaccines induces rejection of subcutaneous and metastatic tumors accompanied by autoimmune depigmentation. *J. Exp. Med.* **190**, 355–366 (1999).
17. C. Twyman-Saint Victor *et al*., Radiation and dual checkpoint blockade activate non-redundant immune mechanisms in cancer. *Nature* **520**, 373–377 (2015).

18. K. D. Moynihan *et al*., Eradication of large established tumors in mice by combination immunotherapy that engages innate and adaptive immune responses. *Nat. Med.* **22**, 1402–1410 (2016).
19. B. Kwong, S. A. Gai, J. Elkhader, K. D. Wittrup, D. J. Irvine, Localized immunotherapy via liposome-anchored Anti-CD137 + IL-2 prevents lethal toxicity and elicits local and systemic antitumor immunity. *Cancer Res.* **73**, 1547–1558 (2013).
20. F. S. Hodi *et al*., Immunologic and clinical effects of antibody blockade of cytotoxic T lymphocyte-associated antigen 4 in previously vaccinated cancer patients. *Proc. Natl. Acad. Sci. U.S.A.* **105**, 3005–3010 (2008).
21. K. D. Moynihan, D. J. Irvine, Roles for innate immunity in combination immunotherapies. *Cancer Res.* **77**, 5215–5221 (2017).
22. B. Kwong, H. Liu, D. J. Irvine, Induction of potent anti-tumor responses while eliminating systemic side effects via liposome-anchored combinatorial immunotherapy. *Biomaterials* **32**, 5134–5147 (2011).
23. J. B. Foote *et al*., A STING agonist given with OX40 receptor and PD-L1 modulators primes immunity and reduces tumor growth in tolerized mice. *Cancer Immunol. Res.* **5**, 468–479 (2017).
24. I. Sagiv-Barfi *et al*., Eradication of spontaneous malignancy by local immunotherapy. *Sci. Transl. Med.* **10**, eaan4488 (2018).
25. A. M. M. Eggermont, M. Crittenden, J. Wargo, Combination immunotherapy development in melanoma. *Am. Soc. Clin. Oncol. Educ. Book.* **38**, 197–207 (2018).
26. A. Ribas *et al*., Oncolytic virotherapy promotes intratumoral T cell infiltration and improves anti-PD-1 immunotherapy. *Cell* **170**, 1109–1119.e10 (2017).
27. T. Tanoue *et al*., A defined commensal consortium elicits CD8 T cells and anti-cancer immunity. *Nature* **565**, 600–605 (2019).
28. M. Milhem *et al*., Intratumoral toll-like receptor 9 (TLR9) agonist, CMP-001, in combination with pembrolizumab can reverse resistance to PD-1 inhibition in a phase Ib trial in subjects with advanced melanoma [Abstract CT-144]. in Clinical Trials (American Association for Cancer Research, 2018), p. CT144.
29. M. Reilley *et al*., Phase 1 trial of TLR9 agonist lefitolimod in combination with CTLA-4 checkpoint inhibitor ipilimumab in advanced tumors. *J. Clin. Oncol.* **37**, TPS2669 (2019).
30. K. J. Harrington *et al*., Preliminary results of the first-in-human (FIH) study of MK-1454, an agonist of stimulator of interferon genes (STING), as monotherapy or in combination with pembrolizumab (pembro) in patients with advanced solid tumors or lymphomas. *Ann. Oncol.* **29** (8), viii712, 10.1093/annonc/mdy424.015 (2018).
31. F. Meric-Bernstam *et al*., Phase Ib study of MIW815 (ADU-S100) in combination with spartalizumab (PDR001) in patients (pts) with advanced/metastatic solid tumors or lymphomas. *J. Clin. Oncol.* **37**, 2507 (2019).
32. H.-J. Schmoll *et al*., Maintenance treatment with the immunomodulator MGN1703, a Toll-like receptor 9 (TLR9) agonist, in patients with metastatic colorectal carcinoma and disease control after chemotherapy: A randomised, double-blind, placebo-controlled trial. *J. Cancer Res. Clin. Oncol.* **140**, 1615–1624 (2014).
33. L. Astor, OS endpoint not met in pivotal phase III CRC IMPALA trial. *Target. Oncol.*, https://www.targetedonc.com/view/os-endpoint-not-met-in-pivotal-phase-iii-crc-impala-trial- (2019).
34. A. Marabelle, H. Kohrt, C. Caux, R. Levy, Intratumoral immunization: A new paradigm for cancer therapy. *Clin. Cancer Res.* **20**, 1747–1756 (2014).
35. A. F. Radovic-Moreno *et al*., Immunomodulatory spherical nucleic acids. *Proc. Natl. Acad. Sci. U.S.A.* **112**, 3892–3897 (2015).
36. D. Shae *et al*., Endosomolytic polymersomes increase the activity of cyclic dinucleotide STING agonists to enhance cancer immunotherapy. *Nat. Nanotechnol.* **14**, 269–278 (2019).
37. H. Liu *et al*., Structure-based programming of lymph-node targeting in molecular vaccines. *Nature* **507**, 519–522 (2014).
38. N. Hanagata, CpG oligodeoxynucleotide nanomedicines for the prophylaxis or treatment of cancers, infectious diseases, and allergies. *Int. J. Nanomedicine* **12**, 515–531 (2017).
39. Y. Ren *et al*., Targeted tumor-penetrating siRNA nanocomplexes for credentialing the ovarian cancer oncogene ID4. *Sci. Transl. Med.* **4**, 147ra112 (2012).
40. Y. Ren, S. Hauert, J. H. Lo, S. N. Bhatia, Identification and characterization of receptor-specific peptides for siRNA delivery. *ACS Nano* **6**, 8620–8631 (2012).
41. Y. Ren, J. E. Sagers, L. D. Landegger, S. N. Bhatia, K. M. Stankovic, Tumor-penetrating delivery of siRNA against TNFα to human vestibular schwannomas. *Sci. Rep.* **7**, 12922 (2017).
42. S. R. Viswanathan *et al*., Genome-scale analysis identifies paralog lethality as a vulnerability of chromosome 1p loss in cancer. *Nat. Genet.* **50**, 937–943 (2018).
43. M.-E. Gilles *et al*., Personalized RNA medicine for pancreatic cancer. *Clin. Cancer Res.* **24**, 1734–1747 (2018).
44. J. H. Lo *et al*., iRGD-guided tumor-penetrating nanocomplexes for therapeutic siRNA delivery to pancreatic cancer. *Mol. Cancer Ther.* **17**, 2377–2388 (2018).
45. T. Tang *et al*., Tumor-specific macrophage targeting through recognition of retinoid X receptor beta. *J. Control. Release* **301**, 42–53 (2019).
46. E. Ruoslahti, Tumor penetrating peptides for improved drug delivery. *Adv. Drug Deliv. Rev.* **110–111**, 3–12 (2017).
47. E. Ruoslahti, S. N. Bhatia, M. J. Sailor, Targeting of drugs and nanoparticles to tumors. *J. Cell Biol.* **188**, 759–768 (2010).
48. M. Pooga, M. Hällbrink, M. Zorko, U. Langel, Cell penetration by transportan. *FASEB J.* **12**, 67–77 (1998).
49. J. H. Lo, E. J. Kwon, A. Q. Zhang, P. Singhal, S. N. Bhatia, Comparison of modular PEG incorporation strategies for stabilization of peptide-siRNA nanocomplexes. *Bioconjug. Chem.* **27**, 2323–2331 (2016).
50. R. Noy, J. W. Pollard, Tumor-associated macrophages: From mechanisms to therapy. *Immunity* **41**, 49–61 (2014).
51. S. Siva, M. P. MacManus, R. F. Martin, O. A. Martin, Abscopal effects of radiation therapy: A clinical review for the radiobiologist. *Cancer Lett.* **356**, 82–90 (2015).
52. S. Demaria *et al*., Ionizing radiation inhibition of distant untreated tumors (abscopal effect) is immune mediated. *Int. J. Radiat. Oncol. Biol. Phys.* **58**, 862–870 (2004).
53. S. Demaria, C. Vanpouille-Box, S. C. Formenti, S. Adams, The TLR7 agonist imiquimod as an adjuvant for radiotherapy-elicited in situ vaccination against breast cancer. *OncoImmunology* **2**, e25997 (2013).
54. E. B. Golden *et al*., Local radiotherapy and granulocyte-macrophage colony-stimulating factor to generate abscopal responses in patients with metastatic solid tumours: A proof-of-principle trial. *Lancet Oncol.* **16**, 795–803 (2015).
55. M. Z. Dewan *et al*., Fractionated but not single-dose radiotherapy induces an immune-mediated abscopal effect when combined with anti-CTLA-4 antibody. *Clin. Cancer Res.* **15**, 5379–5388 (2009).
56. F. Takeshita *et al*., Cutting edge: Role of Toll-like receptor 9 in CpG DNA-induced activation of human cells. *J. Immunol.* **167**, 3555–3558 (2001).
57. C. A. Leifer *et al*., TLR9 is localized in the endoplasmic reticulum prior to stimulation. *J. Immunol.* **173**, 1179–1183 (2004).
58. P. Ahmad-Nejad *et al*., Bacterial CpG-DNA and lipopolysaccharides activate Toll-like receptors at distinct cellular compartments. *Eur. J. Immunol.* **32**, 1958–1968 (2002).
59. L. Hofmann *et al*., Cutaneous, gastrointestinal, hepatic, endocrine, and renal side-effects of anti-PD-1 therapy. *Eur. J. Cancer* **60**, 190–209 (2016).
60. M. Schmidt *et al*., Design and structural requirements of the potent and safe TLR-9 agonistic immunomodulator MGN1703. *Nucleic Acid Ther.* **25**, 130–140 (2015).
61. V. Fogal, L. Zhang, S. Krajewski, E. Ruoslahti, Mitochondrial/cell-surface protein p32/gC1qR as a molecular target in tumor cells and tumor stroma. *Cancer Res.* **68**, 7210–7218 (2008).
62. S. Akira, S. Uematsu, O. Takeuchi, Pathogen recognition and innate immunity. *Cell* **124**, 783–801 (2006).
63. S. Kaczanowska, A. M. Joseph, E. Davila, TLR agonists: Our best frenemy in cancer immunotherapy. *J. Leukoc. Biol.* **93**, 847–863 (2013).
64. A. H. Rahman, D. K. Taylor, L. A. Turka, The contribution of direct TLR signaling to T cell responses. *Immunol. Res.* **45**, 25–36 (2009).
65. T. J. Curiel *et al*., Peptides identified through phage display direct immunogenic antigen to dendritic cells. *J. Immunol.* **172**, 7425–7431 (2004).